The size and dynamics of magnetic flux structures in magnetohydrodynamic turbulence

Axel Brandenburg[a)]
Advanced Study Program & High Altitude Observatory, National Center for Atmospheric Research, P.O. Box 3000, Boulder, Colorado 80307-3000

Itamar Procaccia and Daniel Segel
Department of Chemical Physics, The Weizmann Institute of Science, Rehovot 76100, Israel

(Received 26 October 1994; accepted 4 January 1995)

The structures in magnetohydrodynamic (MHD) flow, flux tubes in particular, are investigated with respect to coherence in the direction of the magnetic field. A length scale, which is interpreted as the diameter of the tubes, is derived from the MHD equations. This scale implies that the tendency towards alignment of flux lines in tubes is a diffusion driven phenomenon. The dynamics of the tubes is also investigated; the major conclusion is that stronger tubes are expected to be straighter. These ideas are tested out on data from numerical simulations of turbulent MHD convection. It is also seen that alignment of flux lines increases with the strength of the tube. Possible reasons for this effect are discussed. © *1995 American Institute of Physics.*

I. INTRODUCTION

In numerical simulations of magnetohydrodynamical (MHD) turbulence the magnetic field generated by dynamo action is typically concentrated in the form of magnetic flux tubes or (less typically) sheets.[1,2] The formation of flux tubes and sheets has also been observed in simulations of ABC flow dynamos.[3] These flux tubes are reminiscent of the vortex tubes that have been seen in large simulations of isotropic turbulence.[4–6] Possibly relevant is that the equation for the evolution of the vorticity in hydrodynamic flow is structurally similar to the equation for the magnetic field in MHD flow: the equations express in both cases the material nature of the field lines and the amplification of the field by the strain.

The tubes are characterized by three length scales – the width of the tube, its curvature and its torsion. One can define the width of these tubes in various ways. The most common is the diameter of tube-like spatial regions in which the field exceeds some threshold value. In hydrodynamics lengths ranging from the Kolmogorov[7] to the Taylor length[5] have been proposed for these tube widths. Such estimates can be made in the following fashion: the equation for the vorticity, $\boldsymbol{\omega}$, in incompressible hydrodynamics is

$$D_t\boldsymbol{\omega}=\mathcal{S}\cdot\boldsymbol{\omega}+\nu\nabla^2\boldsymbol{\omega}, \tag{1}$$

where $\mathcal{S}$ is the strain rate tensor, ν the kinematic viscosity, and $D_t=\partial_t+\mathbf{u}\cdot\nabla$ is the total derivative. It is reasonable to assume that the scale, r_0, of vortex structures in turbulent flows is such that the diffusion down the vorticity gradient balances the strain across the scale that creates the structure. The diffusion term can be estimated as $\nu\omega/r_0^2$. If we estimate the strain by the average dissipation or Kolmogorov scale strain, which is proportional to $\sqrt{\epsilon/\nu}$, where $\epsilon=2\nu\langle\mathcal{S}\rangle^2\approx u_{\rm RMS}^3/L$ is the mean energy flux, L being the external scale, we get the Kolmogorov scale $\ell_K=(\nu^3/\epsilon)^{1/4}$ as r_0. If we estimate the strain as the external strain $u_{\rm RMS}/L$, we get the Taylor microscale $\lambda_K=\sqrt{5}u_{\rm RMS}/\omega_{\rm RMS}$ (Ref. 8) as r_0, where the subscript "RMS" refers to the root mean square value. In terms of the Reynolds number, $\mathrm{Re}=u_{\rm RMS}L/\nu$, these two scales may be written as $\ell_K=L\mathrm{Re}^{-3/4}$ and $\lambda_K=L\mathrm{Re}^{-1/2}$, respectively.

The most thorough study of this question to date was done by Jiménez *et al.*[9] who find the width of a fit to a Gaussian profile for a selection of vortices in flow with $\mathrm{Re}_\lambda=u_{\rm RMS}\lambda_K/\nu$ (i.e. the Reynolds number based on the Taylor microscale) from 35 to 170. They bring evidence indicating that this selection is representative of the entire collection of vortices in the flow. Their conclusion is that the width scales with the Kolmogorov length.

In MHD flows the smallest scale of magnetic flux concentrations, and thus the diameter of the intense flux tubes, is often assumed to be the skin depth, which scales like $\delta=(\eta L/u_{\rm RMS})^{1/2}\sim LR_M^{-1/2}$ with the magnetic Reynolds number $R_M=Lu_{\rm RMS}/\eta$, where η is the magnetic diffusivity. This length scale is motivated from results obtained in the context of two-dimensional magnetic field advection in the presence of laminar flows[10] and low Rayleigh number magneto-convection.[11] For the case $\nu/\eta>1$, the magnetic dissipation scale has been proposed[12,13] to be $\ell_M=(\eta^3/\epsilon)^{1/4}=LR_M^{-3/4}$. The question is whether in turbulent flows the size of the smallest magnetic structures is governed by δ, ℓ_M, or by yet another length scale.

In the following we propose a new relevant length scale which may be motivated by the following argument. In the incompressible case the magnetic field, $\mathbf{B}$, is described by the equation

$$D_t\mathbf{B}=\mathcal{G}\cdot\mathbf{B}+\eta\nabla^2\mathbf{B}, \tag{2}$$

where $\mathcal{G}_{ij}=u_{i,j}$ is the velocity gradient matrix. [Note that, in contrast to the $\mathbf{B}$-field, the $\boldsymbol{\omega}$-field is only governed by the symmetrical part of $\mathcal{G}$, i.e. by the strain $\mathcal{S}=\frac{1}{2}(\mathcal{G}+\mathcal{G}^T)$, since the antisymmetric part can be written as $-\frac{1}{2}\epsilon_{ijk}\omega_k$ which gives $\frac{1}{2}\boldsymbol{\omega}\times\boldsymbol{\omega}=0$.] We can make estimates similar to

[a)]Present address: Nordita, Blegdamsvej 17, DK-2100 Copenhagen Ø, Denmark.

 1070-664X/95/2(4)/1148/9/$6.00

those sketched out above for the direction-coherence length scale in the **B**-field. For the purposes of such an estimate we assume that Kolmogorov scaling ideas still hold for the strain field, which ignores the possible effect of the Lorentz force. If we estimate the strain by the external strain we get the skin depth. In this sense the skin depth is the parallel estimate to the Taylor scale in the hydrodynamic case. If we estimate the strain as the reciprocal of the Kolmogorov estimate of the inertial eddy turnover rate at this length scale (assuming that the scale is in the inertial range) $(\epsilon l^{-2})^{1/3}$ we get the magnetic dissipation scale.[13] If we estimate the strain as the Kolmogorov scale strain we get a length scale

$$r_0 = P_M^{-1/2} \ell_K, \tag{3}$$

where $P_M = \nu/\eta$ is the magnetic Prandtl number. This estimate uses a strain that is the largest of those mentioned, and thus perhaps the most valid for the scale of the strongest structures. If the scale is in the dissipative range (i.e., if $P_M > 1$) it also seems more natural than an inertial or external estimate. No careful study like that of Jiménez *et al.* has been done for MHD flows.

In the present paper we address the issue of flux tube diameter using the definition of tube width used and a formalism recently developed by Constantin *et al.*[14] This method directly uses the equations of motion (in their paper, the Navier–Stokes equation for the dynamics of vorticity in hydrodynamic flow) to produce estimates for the size of vortex tubes as defined by the length scale of the alignment of vorticity vectors. This alternative definition of tube size is motivated by observation in numerical simulations of the high degree of vorticity alignment in tubes. We adapt this view of tubes throughout this paper. The tube size was characterized via well-defined local quantities (essentially derivatives of the field direction). They found that the tube size is proportional to the Kolmogorov scale (or, to be more precise, a local Kolmogorov length). This result both lends rigor to the usual estimate and shows that it holds for this very different definition of tube width as well. It also implies that alignment is a *viscous* phenomenon. The same view is taken here. We use the same formalism to derive a length scale for the typical flux tube size, again defined as the scale of flux line alignment in tubes, which turns out to be equal to the length scale given in (3). No assumptions about the importance of the Lorentz force are necessary. This length scale as the width of flux tubes has not, to our knowledge, been proposed before.

We next address the curvature, through the dynamics of flux tubes, again following Constantin *et al.*[14] We write down an equation for the dynamics of the curvature of a flux tube. This suggests that in addition to the mechanism tending to straighten very strong tubes, parallel to that shown by Constantin *et al.*, in MHD an additional dominant mechanism exists. This is sweeping of the weaker flux tubes around vortex tubes, which could increase the tube curvature and torsion. For completeness we compare to the equations for vortex tubes in MHD flow.

We examine these results using simulations of turbulent MHD convection. The enhanced alignment tendency in stronger flux tubes is confirmed. The scaling for the flux tube widths is naturally harder to confirm given the limited range accessible, but the data are encouraging. We also check numerically some bounds used in our derivation. The straightness of strong tubes is confirmed.

II. FLUX TUBE SCALING

We first show that in regions of strong magnetic field the magnetic field lines tend to align, due to the effect of the magnetic diffusivity. The scale of this alignment will then provide an estimate for the size of magnetic flux tubes.

We define a length scale which characterizes the size of flux tubes by considering the spatial derivatives of the direction of the field. We define a unit vector as $\boldsymbol{\zeta} = \mathbf{B}/B$, where $B = |\mathbf{B}|$, and examine the scale of significant change in the direction of $\boldsymbol{\zeta}$, i.e. $|\nabla \boldsymbol{\zeta}|^{-1}$. In order to be able to estimate this length from the equation of motion, we will average in physical space over a small ball that moves with the fluid, and over an appropriate interval of time.

We thus define a quantity

$$\frac{1}{\lambda_c} = \frac{3}{4\pi r^3 t_r} \int_{|\mathbf{y}| \le r} d\mathbf{y} \int_{t_0}^{t_0+t_r} dt |\nabla \boldsymbol{\zeta}(\mathbf{x}_0 + \mathbf{u}_0 t + \mathbf{y}, t)| \equiv \langle |\nabla \boldsymbol{\zeta}| \rangle_{r,t_r} \tag{4}$$

the average being over a ball B_r of some radius r with mean velocity $\mathbf{u}_0$,

$$\mathbf{u}_0 = \frac{3}{4\pi r^3} \int_{|\mathbf{y}| \le r} \mathbf{u}(\mathbf{x}_0 + \mathbf{y}, t_0) d\mathbf{y}, \tag{5}$$

and over some short time t_r. The choice of r and t_r will be made later.

A first estimate can be made immediately using Cauchy–Schwartz:

$$\frac{1}{\lambda_c} \le \langle B |\nabla \boldsymbol{\zeta}|^2 \rangle_{r,t_r}^{1/2} \left\langle \frac{1}{B} \right\rangle_{r,t_r}^{1/2}. \tag{6}$$

To estimate the first of the factors in this upper bound we use the method used in Constantin *et al.*[14] and the inequalities therein. This factor is estimated by comparing terms in the MHD equation of motion for B,

$$D_t B = (\beta - \eta |\nabla \boldsymbol{\zeta}|^2) B + \eta \nabla^2 B, \tag{7}$$

where β is the diagonal component in the field direction of the strain tensor $\mathcal{S}$, $\beta = \boldsymbol{\zeta} \cdot \mathcal{S} \cdot \boldsymbol{\zeta}$. We perform the averages over the ball by use of a cutoff function $\phi(\mathbf{x},t) = \phi_0[(\mathbf{x} - \mathbf{x}_0 - \mathbf{u}_0 t)/r]$ where the function ϕ_0 is such that $\phi_0(\mathbf{y}) = 1$ for $|\mathbf{y}| < 1/2$, $\phi_0(\mathbf{y}) = 0$ for $|\mathbf{y}| > 1$, and $\phi_0(\mathbf{y})$ is monotonic and smooth enough in $1/2 \le |\mathbf{y}| \le 1$ to have smooth derivatives.

Multiplying (7) by ϕ and integrating we have an equation for the desired average

$$\eta \int d\mathbf{x} B |\nabla \boldsymbol{\zeta}|^2 \phi = \int d\mathbf{x} \beta B \phi - \frac{d}{dt} \int d\mathbf{x} B \phi + \int d\mathbf{x} \times \left[\left(\frac{\partial}{\partial t} + \mathbf{u} \cdot \nabla - \eta \nabla^2 \right) \phi \right] B. \tag{8}$$

We now use

$$\left(\frac{\partial}{\partial t}+\mathbf{u}\cdot\nabla-\eta\nabla^2\right)\phi=\frac{\mathbf{u}-\mathbf{u}_0}{r}\cdot\nabla\phi_0-\frac{\eta}{r^2}\nabla^2\phi_0 \tag{9}$$

to write

$$\langle B|\nabla\zeta|^2\rangle_{r,t_r}=\frac{1}{\eta}(T_1+T_2+T_3+T_4), \tag{10}$$

where

$$T_1=\frac{1}{r^3t_r}\int_{t_0}^{t_0+t_r}dt\int d\mathbf{x}\beta B\phi_0, \tag{11}$$

$$T_2=\frac{1}{r^3t_r}\int_{t_0}^{t_0+t_r}dt\left(-\frac{d}{dt}\int d\mathbf{x}B\phi_0\right)r, \tag{12}$$

$$T_3=\frac{1}{r^3t_r}\int_{t_0}^{t_0+t_r}dt\int d\mathbf{x}\left(\frac{\mathbf{u}-\mathbf{u}_0}{r}\cdot\nabla\phi_0\right)B, \tag{13}$$

$$T_4=\frac{\eta}{r^5t_r}\int_{t_0}^{t_0+t_r}dt\int d\mathbf{x}B\nabla^2\phi_0. \tag{14}$$

We now denote averaging over the moving ball of some f as $\langle f\rangle_{r,t}$, and use the fact that $\langle|\nabla\phi_0|\rangle_{r,t}\leq C_1/r$ and $\langle\nabla^2\phi_0\rangle_{r,t}\leq C_2/r^2$, C_1 and C_2 constants of order unity. This allows us to give the simpler estimate

$$\langle B|\nabla\zeta|^2\rangle_{r,t_r}\leq\frac{1}{\eta}(I+II+III+IV) \tag{15}$$

where

$$I=\langle|\beta|B\rangle_{r,t_r}, \tag{16}$$

$$II=\frac{C_0}{r^3t_r}\int_{|\mathbf{y}|<r}d\mathbf{y}B(\mathbf{y},t_0), \tag{17}$$

$$III=\frac{C_1}{r}\langle|\mathbf{u}-\mathbf{u}_0|B\rangle_{r,t_r}, \tag{18}$$

$$IV=\frac{C_2\eta}{r^2}\langle B\rangle_{r,t_r}. \tag{19}$$

We now use the inequality

$$\beta^2\leq|\nabla\mathbf{u}|^2, \tag{20}$$

β being just one of the components of the strain tensor. This bound may not be sharp since the geometric factor involved may depend on the Reynolds number, through alignment: if with increasing Reynolds number the vorticity has an increasing tendency to align with the intermediate strain eigenvalue, as has been suggested,[5] $\beta/|\nabla\mathbf{u}|$ will decrease with Re.

We now define

$$A\equiv\langle|\nabla\mathbf{u}|^2\rangle_{r,t_r}^{1/2}\langle B^2\rangle_{r,t_r}^{1/2}; \tag{21}$$

A will serve as a bound for all four terms. Using (20) we have by Cauchy–Schwartz

$$I\leq A. \tag{22}$$

Now using the Poincaré inequality

$$\int_{|\mathbf{x}|\leq r}d\mathbf{x}|\mathbf{u}-\mathbf{u}_0|^2\leq r^2\int_{|\mathbf{x}|\leq r}d\mathbf{x}|\nabla\mathbf{u}|^2 \tag{23}$$

we have in addition, again by Cauchy–Schwartz

$$III\leq C_1A. \tag{24}$$

This bound does not include a geometric factor, since it includes an integral over all directions. The Poincaré inequality should be quite sharp here since at the scale r, which is small as we will see, we expect the field to be quite smooth. Therefore this term will dominate I if the latter indeed decreases with Reynolds number.

The terms II and IV can be bounded by A by making a choice of the ball size r and the averaging time t_r. The time t_r is fixed by demanding that $II\leq C_0A$. This translates to the condition

$$t_r\geq\frac{3}{4\pi r^3}\frac{\int_{|\mathbf{y}|<r}d\mathbf{y}[B(\mathbf{y},t_0+t_r)-B(\mathbf{y},t_0)]}{\langle|\nabla\mathbf{u}|^2\rangle_{r,t_r}^{1/2}\langle B^2\rangle_{r,t_r}^{1/2}}. \tag{25}$$

This is an implicit equation giving a lower bound t_{r_0} for t_r unless the RHS is proportional to t_r, i.e. when B has a constant growth rate. However in this latter case the growth rate is bounded by β [see Eq. (7)] and we can bound II by A for any t_r.

We obtain the ball size r by demanding that IV is bounded by C_2A. In fact we demand the more stringent condition that

$$IV<C_2\frac{\eta}{r^2}\langle B^2\rangle_{r,t_r}^{1/2}\leq C_2A \tag{26}$$

which means we must have

$$r\geq C_2^{1/2}r_0\equiv C_2^{1/2}\frac{\eta^{1/2}}{\langle|\nabla\mathbf{u}|^2\rangle_{r,t_r}^{1/4}}. \tag{27}$$

We can use r_0 to form a time scale:

$$\tau=\frac{1}{\langle|\nabla\mathbf{u}|^2\rangle_{r,t_r}^{1/2}}=\frac{r_0^2}{\eta}. \tag{28}$$

This is just the strain time scale (by the first definition) or magnetic field diffusion time over the distance r_0 (by the second definition), which are the same at this scale. So since the scale of the structures will turn out to be proportional to r_0, this scale can be seen as being determined by the requirement that the magnetic field dissipates away just at the rate that the strain builds it up.

Finally we note that if the flow is compressible a term $-(\nabla\cdot\mathbf{u})B$ is added to the equation for B. This would add to (15) for $\langle B|\nabla\zeta|^2\rangle$ a term

$$V=\langle|\nabla\cdot\mathbf{u}|B\rangle_{r,t_r}. \tag{29}$$

This is easily bounded by A since $\langle B\rangle\leq\langle B^2\rangle^{1/2}$ and $\langle|\nabla\cdot\mathbf{u}|\rangle\leq\langle|\nabla\mathbf{u}|\rangle\leq\langle|\nabla\mathbf{u}|^2\rangle^{1/2}$. So our derivation holds for the compressible case too.

Summing up the results obtained so far we conclude that

$$\langle B|\nabla\zeta|^2\rangle_{r_0,t_{r_0}} \leq \frac{C_3}{\eta r_0^3 t_{r_0}}\left(\int_0^{t_{r_0}} dt \int_{|\mathbf{x}|\leq r_0} d\mathbf{x}|\nabla\mathbf{u}|^2\right)^{1/2} \times\left(\int_0^{t_{r_0}} dt \int_{|\mathbf{x}|\leq r_0} d\mathbf{x}B^2\right)^{1/2}, \tag{30}$$

where $C_3 = 1 + C_0 + C_1 + C_2$.

This certainly is a finite bound: we can easily give a (far from sharp) bound in terms of ϵ, the mean energy flux of kinetic energy per unit time and mass,

$$\epsilon = \frac{\nu}{L^3}\int_{|\mathbf{x}|\leq L} d\mathbf{x}|\nabla\mathbf{u}|^2 \tag{31}$$

and the total magnetic energy

$$E_B = \frac{1}{8\pi}\int_{|\mathbf{x}|\leq L} d\mathbf{x}B^2. \tag{32}$$

We can now estimate λ_c. We assume that

$$\left\langle \frac{1}{B} \right\rangle_{r,t_r} \langle B^2\rangle_{r,t_r}^{1/2} \leq C_4 \tag{33}$$

since we are interested in areas of high B where $\langle 1/B \rangle$ does not blow up, and we can bound $\langle B^2\rangle_{r,t_r}$ in terms of the magnetic energy which is always bounded. Now using the estimates (30) and (33) in (6) we find

$$\lambda_c \leq C_3 C_4 r_0. \tag{34}$$

The length scale r_0 is easily related to the usual Kolmogorov length scale

$$\ell_K \sim \left(\frac{\nu^3}{\epsilon}\right)^{1/4}. \tag{35}$$

This scale differs from the scale found here in that it includes ν^3 instead of η^3 and in that it includes the kinetic dissipation averaged over the whole system instead of just over the ball B_r. This scale can vary from place to place in the flow, dependent on the size of the dissipation averaged over the ball and on its radius r_0. In general we would assume that the local averaging does not make too much of a difference. Because the dependence of the length scales is on $\epsilon^{1/4}$, a very large deviation from the average dissipation in the ball is necessary for the length scale to be significantly different.

At any rate, denoting the locally averaged Kolmogorov scale as $\ell_K(\mathbf{x})$, λ_c can be estimated up to a constant of order one as

$$\lambda_c \sim \ell_K(\mathbf{x}) P_M^{-1/2}, \tag{36}$$

if we assume that our bound is sharp as far as scaling is concerned (this issue is considered in Sec. IV). If we consider the average size of tubes, what we propose here is that the characteristic size for flux structures in MHD turbulent flow is a new length scale, equal up to a numerical constant to $L\mathrm{Re}^{-3/4}P_M^{1/4}$. It thus differs from other length scales proposed, such as the dissipation length $\ell_M \sim LR_M^{-3/4}$ or the skin depth $\delta \sim LR_M^{-1/2}$, in varying with Prandtl number for constant R_M. Furthermore, we have seen an intuitive description of this scale—just as the Kolmogorov length (the scale of vortex tubes in Navier–Stokes flow) is the scale where the average strain time scale (at this scale also the eddy turnover time) is equal to the viscous diffusion time over that scale—here the new scale is that where the eddy turnover time is equal to the magnetic diffusion time.

III. CURVATURE DYNAMICS

One can write down the equations for the evolution of the curvature of a flux tube in a strain field, or more precisely of the flux lines making it up, in a straightforward manner from the MHD equations. We look only at the nondiffusive dynamics and in this section take $\eta = 0$, assuming that the role of the viscosity lies primarily not in the dynamics of the geometry of the tubes but in allowing their coherence, as described in Sec. II. In fact these equations hold for any material line (as a flux line is in MHD when diffusion is neglected) in a strain field. Such an equation was derived by Drummond and Münch[15] for material lines and in a somewhat different form in Constantin *et al.*[14] for vorticity lines. We will follow the second paper's method and form; the differences between them are discussed in Ref. 14.

The flux lines are defined as having at every point the direction ζ. From the diffusionless equation for the field

$$D_t\mathbf{B} = \mathcal{S}\cdot\mathbf{B}, \tag{37}$$

and (7) we find that

$$D_t\boldsymbol{\zeta} = (\mathcal{S} - \beta\mathbf{I})\cdot\boldsymbol{\zeta}. \tag{38}$$

Using the identity $\mathcal{G}_{ij} = \mathcal{S}_{ij} - \frac{1}{2}\epsilon_{ijk}\omega_k$ we can also write (4) as

$$D_t\boldsymbol{\zeta} = (\mathcal{S} - \beta\mathbf{I})\cdot\boldsymbol{\zeta} + \tfrac{1}{2}\boldsymbol{\omega}\times\boldsymbol{\zeta}. \tag{39}$$

The vorticity rotates the magnetic field vector as it convects the magnetic field around it.

We now choose to work in the Frenet local coordinates for a vorticity field. In these, one coordinate is that in the direction of the field, with a unit vector we have defined as $\boldsymbol{\zeta}$, another by the direction of curvature of these unit vectors, with unit vector $\mathbf{n}$, and completed by the binormal $\mathbf{b}$. These satisfy

$$(\boldsymbol{\zeta}\cdot\nabla)\begin{pmatrix}\boldsymbol{\zeta}\\ \mathbf{n}\\ \mathbf{b}\end{pmatrix} = \begin{pmatrix} 0 & 1/\rho & 0\\ -1/\rho & 0 & T\\ 0 & -T & 0\end{pmatrix}\begin{pmatrix}\boldsymbol{\zeta}\\ \mathbf{n}\\ \mathbf{b}\end{pmatrix}, \tag{40}$$

where $\rho = |(\boldsymbol{\zeta}\cdot\nabla)\boldsymbol{\zeta}|^{-1}$ is the local radius of curvature and $T = \mathbf{b}\cdot(\boldsymbol{\zeta}\cdot\nabla)\mathbf{n}$ the local torsion of the field. In this frame the stretching vector of the flux line, $\boldsymbol{\zeta}\cdot\mathcal{S}$ has three components, one being the stretching factor β and the other two $\mathcal{S}_n = \boldsymbol{\zeta}\cdot\mathcal{S}\cdot\mathbf{n}$ and $\mathcal{S}_b = \boldsymbol{\zeta}\cdot\mathcal{S}\cdot\mathbf{b}$. Now using the useful formula[14] for the operator commutator

$$[D_t, (\boldsymbol{\zeta}\cdot\nabla)] = -\beta(\boldsymbol{\zeta}\cdot\nabla) \tag{41}$$

we find after a little algebra the equation for the flux line radius of curvature

$$D_t\rho = [\beta - \rho(\boldsymbol{\zeta}\cdot\nabla)\mathcal{S}_n + \rho T\mathcal{S}_b]\rho. \tag{42}$$

Again using the decomposition of $\mathcal{S}$ into strain and vorticity this can be written as

$$D_t\rho=[\beta-\rho(\boldsymbol{\zeta}\cdot\nabla)(\mathcal{S}_n-\tfrac{1}{2}\omega_b)+\rho T(\mathcal{S}_b+\tfrac{1}{2}\omega_n)]\rho, \tag{43}$$

where $\omega_n=\boldsymbol{\omega}\cdot\mathbf{n}$ and $\omega_b=\boldsymbol{\omega}\cdot\mathbf{b}$. This equation shows the effect of a velocity field on the curvature in terms of the strain and vorticity and the geometry of the magnetic field only. The stretching β pulls on the flux line at both ends and thus straightens it. The "force" on the tube in the direction of the curvature is given by the strain $\mathcal{S}_n$ and the convection of the vorticity component ω_b. If this varies along the flux line it will bend it. If the line has torsion or a helical structure, lying locally on a cylinder, the direction $\mathbf{b}$ is on the cylinder normal to the line. The "force" along the helix cylinder is given by the strain $\mathcal{S}_b$ and the convection of the vorticity component ω_n. A positive force extends the helix along the cylinder and thus reduces the curvature.

Note that the first term here is just the same as the right hand side in the equation for B. Since this is the homogeneous (linear in curvature) term in our equation, we might expect that at least initially the same strain that creates the strong flux tubes would tend to straighten them out. The strong magnetic fields were created by a strong stretching rate β coherent over some time. We would thus also expect that since in a rapidly varying field one would not expect that other quantities would be coherent over the creation time in the same regions, the term with β would dominate.

However things are not that simple. The equation Drummond and Münch derive, when put in our terms, is

$$D_t\rho=(2\beta-\mathbf{n}\cdot\mathcal{S}\cdot\mathbf{n})\rho-\rho^2\sum\mathcal{H}_{ijk}\zeta_i\zeta_j n_k \tag{44}$$

where $\mathcal{H}_{ijk}$ is the third rank tensor $\mathcal{H}_{ijk}=\partial^2 u_i/\partial x_j\partial x_k$. A little manipulation shows that these two equations are in fact the same, due to the identity

$$\sum\mathcal{H}_{ijk}\zeta_i\zeta_j n_k=(\boldsymbol{\zeta}\cdot\nabla)\mathcal{S}_n-\frac{1}{\rho}\mathbf{n}\cdot\mathcal{S}\cdot\mathbf{n}+\frac{1}{\rho}\beta-T\mathcal{S}_b. \tag{45}$$

Drummond and Münch, too, assume that the homogenous term will dominate the early evolution, and that the term including the strong β will dominate. However both these concepts become ill-defined given the identities just mentioned.

In fact the concept of a homogeneous term is a statistical matter. The separation of such a term from the rest of the equation is valid only when it is weakly correlated with the other terms through the process under discussion. In a real turbulent flow the local structure of the flow may well introduce correlations that will make relations like (45) significant. If our expectation, based on our equation, is correct, the tube will straighten at the same rate as its magnetic field grows. If the situation is closer to that suggested by Drummond and Münch, the tube straightens out too; since the diagonal strain component in the direction of the flux tube must be larger than any other diagonal strain component (which did not create a flux tube) such as $\mathbf{n}\cdot\mathcal{S}\cdot\mathbf{n}$, the rate at which the tube straightens is faster than that at which the field grows. At any rate we would expect that the strong flux tubes be quite straight. The difference between the equations is discussed more fully in Ref. 14.

All this should hold only during the time in which the tube is created. When the growth rate strain β starts to fade, other terms can become important or even dominant. One term in particular can be seen in action in the simulations[2]: strong vortex tubes can be seen to wrap flux tubes or filaments around them, thus increasing their curvature. However these processes would tend to act more strongly on weak and small structures, and act on them in later stages of their evolution, where their strength has begun to dissipate. Therefore, we still would expect to see that the strongest flux tubes are relatively straight. We cannot rule out, however, nonlinear feedback processes in which tubes (of both flux and vortex lines) interact and amplify each other while wrapping one about the other.

For completeness we bring the equations governing curvature of vortex lines in MHD, for comparison to flux tubes in MHD and to Navier–Stokes vortex tubes. In MHD an added term which we call $\mathbf{F}$ is added to the equation for the vorticity:

$$D_t\boldsymbol{\omega}=\mathcal{S}\cdot\boldsymbol{\omega}+(\mathbf{B}\cdot\nabla)\mathbf{J}+(\mathbf{J}\cdot\nabla)\mathbf{B}\equiv\mathcal{S}\cdot\boldsymbol{\omega}+\mathbf{F}. \tag{46}$$

The equation for the curvature of the vortex filaments is now

$$D_t\rho=\left[\alpha-\rho(\boldsymbol{\xi}\cdot\nabla)\left(\mathcal{S}_n+\frac{F_n}{\omega}\right)+\rho T\left(\mathcal{S}_b+\frac{F_b}{\omega}\right)\right]\rho, \tag{47}$$

parallel to the equation for flux curvature above, where $\boldsymbol{\xi}$ is the vorticity direction vector (analogous to $\boldsymbol{\zeta}$), α is the vorticity stretching rate (analogous to β), the strain rate along the vortex line $\alpha=\boldsymbol{\xi}\cdot\mathcal{S}\cdot\boldsymbol{\xi}$, and where F_n and F_b are the components of $\mathbf{F}$ in the normal and bi-normal directions respectively. The new terms express the influence of the magnetic field on the vortex lines, including the nonlinear processes mentioned.

IV. NUMERICAL SIMULATIONS

Numerical simulations of three-dimensional MHD turbulence allow us to test some of the predictions made above regarding the size and dynamics of magnetic flux structures.[16] Such simulations can furthermore be used to check our analysis by determining the sharpness of various bounds used above. We use data of MHD turbulence that had originally been produced to gain some understanding of the solar magnetic field. These simulations contain therefore additional physics such as a rotating frame (Coriolis force), stratification (with density ratio 1:20 to 1:80), and convective overshoot into a lower stably stratified layer. We cannot rule out the possibility that the particular physics involved will affect our conclusion, but nothing in the analysis given here seems to suggest that possibility. We therefore only refer to the original paper[2] for more details.

The analysis of flux tubes in Sec. II only applies to those regions in space where the magnetic field is strong. We therefore adopt averages, $\langle\ldots\rangle_B$, which are performed over those points in space where the magnetic field exceeds a certain

TABLE I. The coefficients in Eqs. (49)–(51) for various runs at different Reynolds number and numerical resolution. (Further properties of these runs are given in Table II.)

Case	O	A	B	C	D
Mesh	$126^2\times105$	$63^2\times63$	$95^2\times63$	$126^2\times105$	$126^2\times105$
Re	140	310	540	1100	1200
(49)	0.835	0.858	0.877	0.837	0.832
(50)	0.054	0.034	0.027	0.043	0.050
(51)	1.06	1.05	1.08	1.10	1.11

threshold (typically 3 times the RMS value of B). In accordance with (4), we define a statistical measure of λ_c as

$$\lambda_c^{-1}=\langle|\nabla\zeta|\rangle_B. \tag{48}$$

We have a basic problem in that while our theoretical conclusions hold for the highest field regions, these regions have rather few points in them, leading to poor statistics. The threshold chosen is a compromise between these demands.

We first use the numerics to test out our argument by examining the sharpness of the bounds used. The data show that the bound in (6) is consistently nearly saturated, i.e.

$$\langle|\nabla\zeta|\rangle_B\approx(0.8\ldots0.9)\langle B|\nabla\zeta\rangle|^2{}_B^{1/2}\langle B^{-1}\rangle_B^{1/2}. \tag{49}$$

Another inequality was used in (20), and it turns out that this is not a sharp bound, but that typically

$$\langle\beta^2\rangle_B\approx(0.03\ldots0.05)\langle|\mathbf{\nabla u}|^2\rangle_B. \tag{50}$$

This bound appears as one of a series bounding all the terms of the equation for B uniformly; since it appears additively the lack of sharpness is not important. The data indicate that the constant in (33) is consistently close to unity, i.e.

$$\langle B^{-1}\rangle_B\langle B^2\rangle_B^{1/2}\approx1.0\ldots1.1. \tag{51}$$

In Table I we give the coefficients in (49)–(51). These coefficients do not seem to depend significantly on Re or on the numerical resolution used.

An important question concerns the scaling of the thickness of magnetic structures, λ_c, with the kinetic and magnetic Reynolds numbers. We are especially interested in whether λ_c scales with the newly introduced length scale r_0, or rather with the more traditional magnetic skin depth scale, δ, or the magnetic dissipation scale ℓ_M. Unfortunately, this is not easy to check, because the scaling of these length scales with Re and R_M is not very different. Supposing that $\ell_M\sim L\mathrm{Re}^{-3/4}$ is valid for our low Reynolds number simulations too, we expect $\lambda_c\sim r_0\sim L\mathrm{Re}^{-3/4}P_M^{-1/2}$, which differs from the skin depth scaling, $\delta\sim L\mathrm{Re}^{-1/2}P_M^{-1/2}$, by a factor $\mathrm{Re}^{1/4}$. For convection, the range of different Re accessible is limited between about 200 (for the flow to be sufficiently turbulent) and 1000 (compatible with the highest resolution presently available). In addition, our remarks in the Introduction indicate that it is possible that there is a crossover from our length scale to the magnetic dissipation length at $P_M=1$, just around where most of our results are centered. Given all these limitations we must consider our results as preliminary.

In Fig. 1 we plot $\log_{10}\lambda_B P_M^{1/2}$ versus $\log_{10}\mathrm{Re}$. Although the scatter is considerable, the slope in this plot appears to be closer to $-3/4$ rather than $-1/2$, suggesting that the scaling of λ_c may indeed be governed by r_0 rather than by the skin depth δ. From Fig. 1 we see that λ_c also agrees reasonably with $\ell_M=LR_M^{-3/4}$. The case with $P_M=4$ (Run A) does indeed not satisfy this relation.

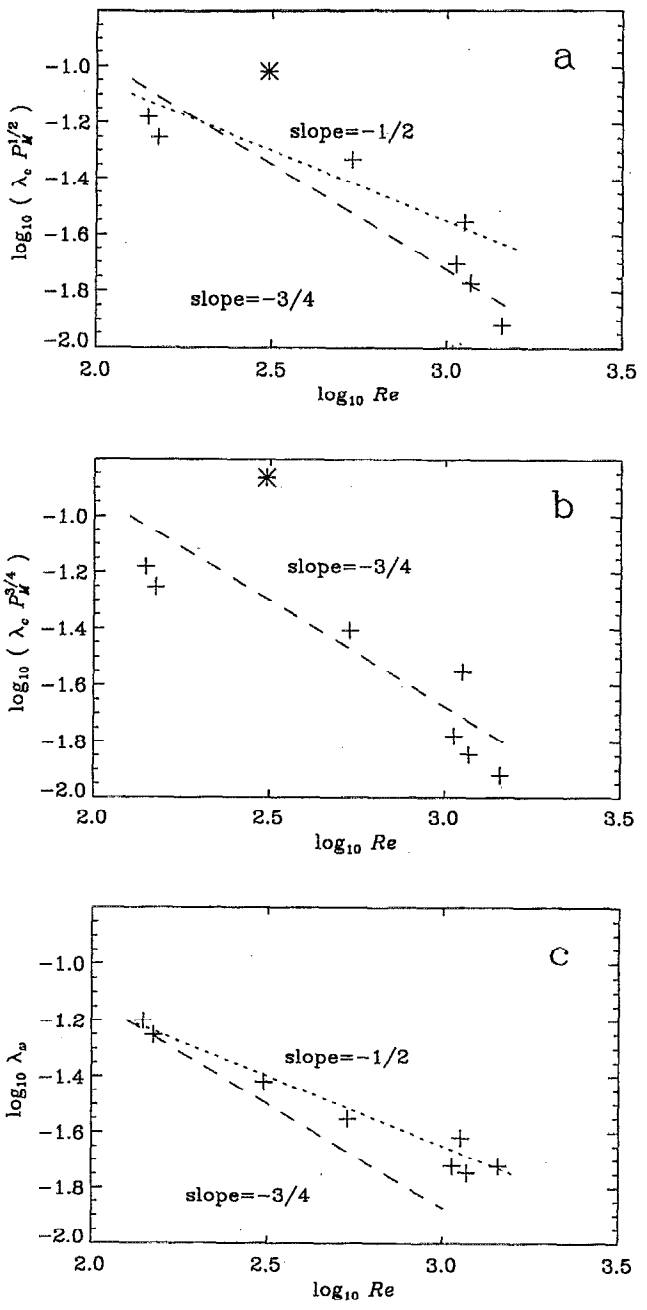

FIG. 1. Scaling of the sizes of flux tubes [(**a**) and (**b**)] and vortex tubes (**c**) versus Reynolds number in turbulent MHD convection. The asterisks in the first two panels indicates Run A for which $P_M=4$. All other runs are denoted by a plus sign ($P_M\leqslant1$).

We also plot the thickness of the vortex tubes, using the definition (4) for the vorticity field instead of the magnetic field. We do not have a bound for this width, λ_ω, in the MHD case. Constantin *et al.*, as we said above, derive a bound in the pure Navier–Stokes case which scales as

TABLE II. Summary of data from numerical simulations.

Case	O	A	B	C	D
Mesh	$126^2\times105$	$63^2\times63$	$95^2\times63$	$126^2\times105$	$126^2\times105$
Re	140	310	540	1100	1200
R_M	140	1240	270	1100	600
P_M	1.0	4.0	0.5	1.0	0.5
Re_λ	35	63	89	121	123
δx	0.016	0.032	0.032	0.016	0.016
λ_K	0.252	0.199	0.165	0.101	0.105
λ_M	0.055	0.076	0.065	0.029	0.027
δ	0.085	0.028	0.061	0.030	0.041
$\ell_K(\mathbf{x})P_M^{-1/2}$	0.020	0.006	0.013	0.006	0.006
r_0	0.025	0.007	0.013	0.005	0.007
λ_c	0.063	0.048	0.066	0.028	0.024
ρ	0.302	0.272	0.292	0.154	0.104
$1/T$	0.069	0.029	0.049	0.023	0.022

$L\mathrm{Re}^{-3/4}$. If we would assume that the influence of the magnetic field and current on the vortex tubes is small—the regions in which each are strong tend to be quite different—we would take this scale as a first estimate for the tube widths. We plot the tube width vs Re in Fig. 1(c). These results point toward a dependence on the Taylor scale that scales as $L\mathrm{Re}^{-1/2}$. This could be due to the effects of stratification and rotation, but it might also suggest that the assumption that the magnetic field is unimportant for the size of vortex tubes can not be justified in the present case.

In Table II we also give the curvature radius ρ and the torsion scale $1/T$.[17] In the table, δx is the mesh size, and $\lambda_M=\sqrt{5}B_{\mathrm{RMS}}/J_{\mathrm{RMS}}$ is the magnetic Taylor microscale. The quantity $\ell_K(\mathbf{x})$ has here been estimated as $(\nu^2/\langle|\nabla\mathbf{u}|^2\rangle_B)^{1/4}$. The curvature radius is typically 2–4 times larger than λ_c. Note, however, that in all cases λ_c is comparable to the mesh size δx, and one should therefore consider them with care. On the other hand, we should emphasize that, although the value of λ_c is generally much closer to δ than to r_0, it is the *dependence* on the Reynolds number that is important to us here. In other words, the scale of flux structures is expected to be r_0 times some coefficient. Our data suggest $\lambda_c\approx3r_0$. Further, notice that the torsion scale is typically shorter than the curvature radius. This is perhaps somewhat surprising, but one should mention the possibility that our torsion scale captures not only the global structure of tubes, but also the intrinsic torsion within a tube. Thus, even if a tube was straight, it might still have intrinsic torsion, due to winding of flux lines within the tube, which would be measured by our $1/T$ scale.

In Fig. 2 we show the dependence of the tube thickness on the threshold value. The results show clearly that in regions of strong magnetic field the tubes are "thicker," in the sense of having a much stronger tendency towards alignment. For comparison, we also show the corresponding thickness of vortex tubes. Clearly, the tubes are thicker in regions of strong vorticity. This striking phenomenon has several possible explanations. The first is suggested by our own estimate (27)—if the dissipation goes down with field strength the alignment scale should go up. This might be explained by regions having weak fields due to the action of

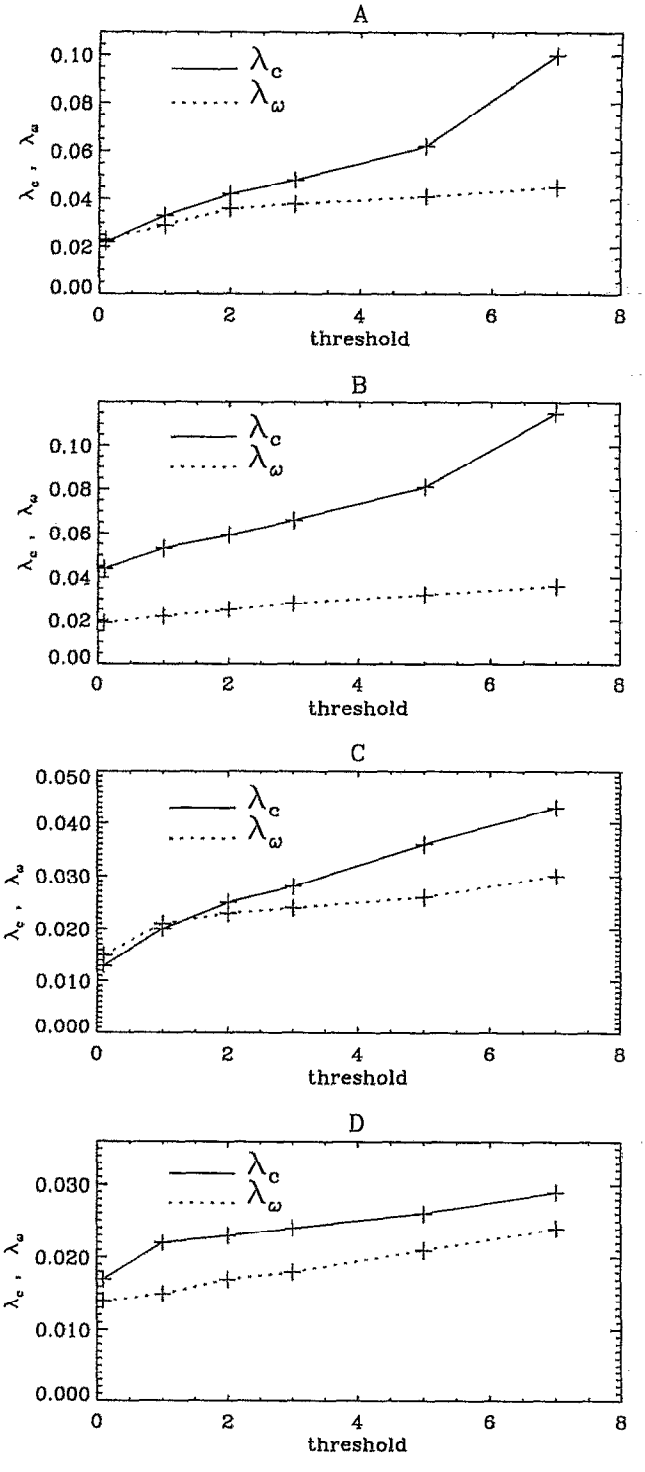

FIG. 2. Scaling of the sizes of flux tubes (solid lines) and vortex tubes (dotted lines) versus the threshold values of B and ω, respectively, for the different runs of turbulent MHD convection.

strong dissipation. However from Fig. 3 we can see that this is far from explaining the results—any effect is greatly attenuated by the weak power (1/4) of the dissipation in the length scale estimate, $\ell_K(\mathbf{x})=(\nu^2/\langle|\nabla\mathbf{u}|^2\rangle_B)^{1/4}$. Another explanation is offered by the analysis of the effects of viscosity on vortex lines presented in Constantin *et al.* (In the MHD

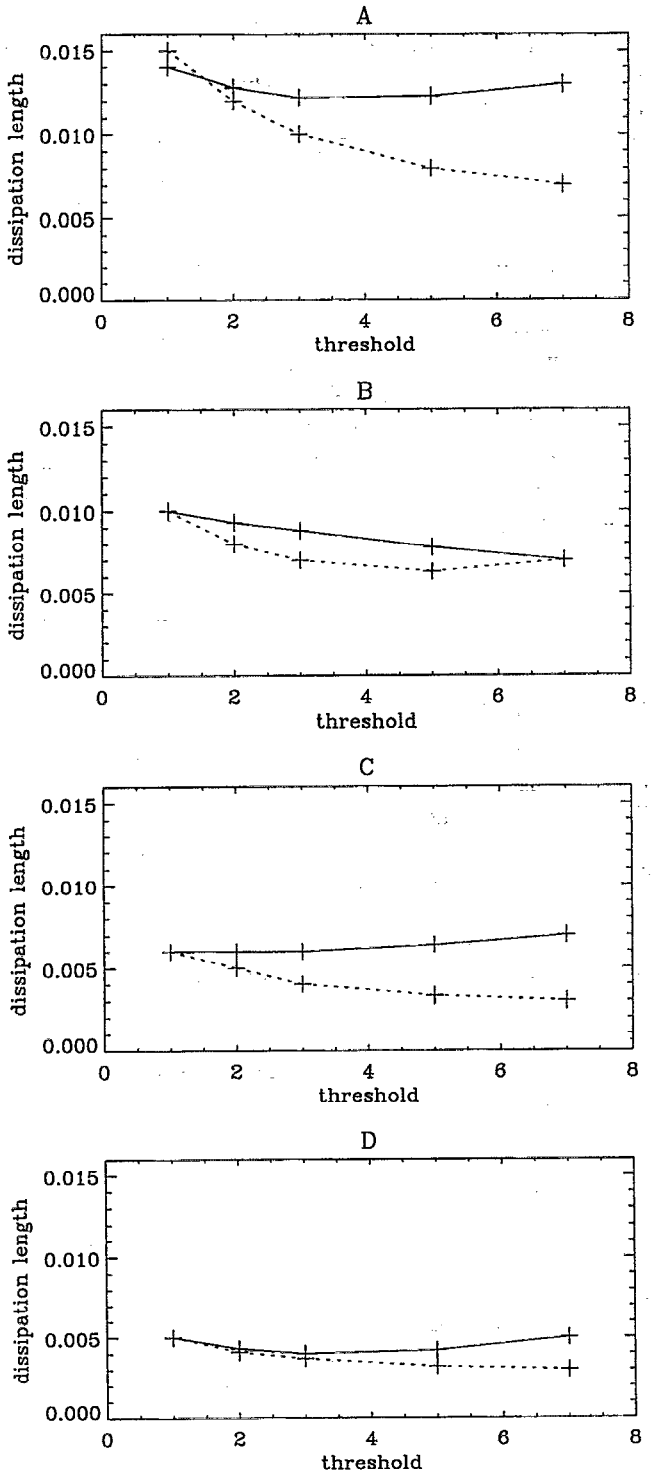

FIG. 3. Scaling of the dissipation lengths versus the threshold value of the magnetic field (solid lines) and the vorticity (dotted lines) for the different runs of turbulent MHD convection.

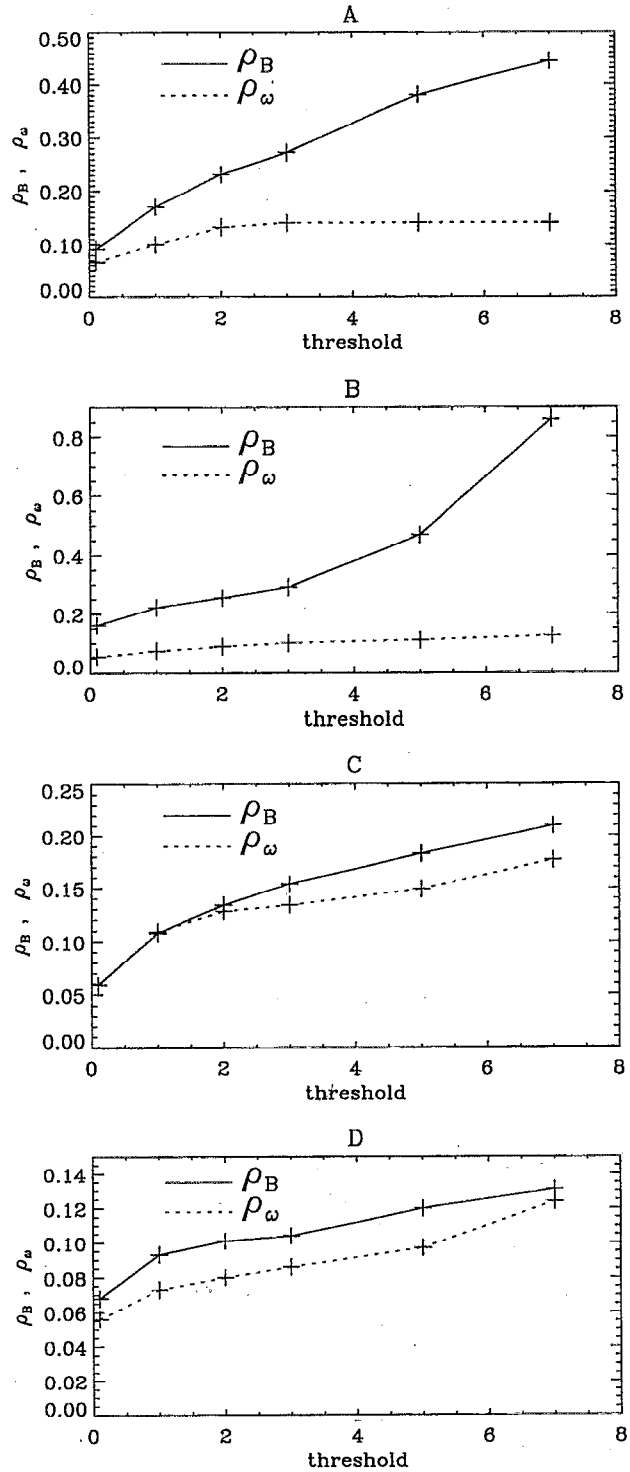

FIG. 4. Scaling of the curvature radii of flux tubes (solid lines) and vortex tubes (dotted lines) versus the threshold values of B and ω, respectively, for the different runs of turbulent MHD convection.

case the magnetic diffusivity acting on the magnetic field would play the role of the viscosity on vorticity.) They show that the viscosity has the effect of aligning weaker vectors with stronger vectors, causing alignment in tubes with very strong cores. A third mechanism is strain with direction coherent in space and time amplifying a given field component, thus causing strong fields in a given direction. This would only work if the created tube stays straight through its creation. The final explanation could well stem from a combination of these and other, as yet unknown, factors.

The curvature radius scales with the threshold value in a similar manner as the tube thickness; see Fig. 4. This is in

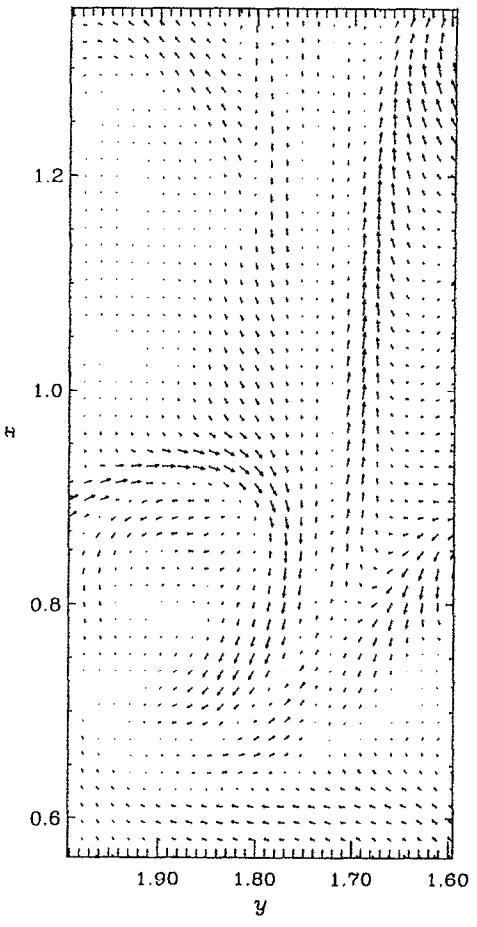

FIG. 5. Vectors of the magnetic field in a small two-dimensional slice for Run D. Note the occurrence of both curved and straight **B**-tubes.

complete agreement with our analysis of tube dynamics in Sec. III.

In order to gain further information about the importance of the second and third strain terms in (42) we determine the correlation $C=\langle\beta\gamma\rangle_B/(\langle\beta^2\rangle_B\langle\gamma^2\rangle_B)^{1/2}$, where $\gamma=-\rho(\boldsymbol{\zeta}\cdot\mathbf{\nabla})\mathcal{S}_n+\rho T\mathcal{S}_b$. We find values around ± 0.05, indicating that the γ terms are indeed of little importance, and that the curvature radius ρ grows at the *same* rate β at which flux tubes are stretched. Furthermore, we find that the $\boldsymbol{\omega}$-terms in (43) are approximately as important as the $\mathcal{S}$-terms. This indicates that the **B**-vectors do indeed experience considerable bending by the vortex field. An analogous mechanism for the $\boldsymbol{\omega}$-tubes does not exist, which is probably the reason why $\boldsymbol{\omega}$-tubes are typically straight, whereas **B**-tubes are not.

Finally, we show in Fig. 5 an example of a flux tube from Run D. Note the alignment of the **B**-vectors with the general orientation of the tube.

V. CONCLUSIONS

In this paper we have investigated two length scales characterizing flux tubes in MHD flow. We estimate the diameter of the tubes and derive a length scale at which the strain builds up the structures at the same rate that the diffusion breaks them down. While scaling is hard to verify with the range of scales accessible by numerical simulations, the numerical data show some support for this claim.

Our estimate for the tube widths is meant to describe the average size of these tubes, in particular with respect to their scaling with relevant dimensionless numbers, P_M and R_M. However it turns out that it is not refined enough to describe the differences between different tubes in the same simulation. Simulations show a strong increase towards alignment for stronger flux tubes. A possible explanation is given by a recent analysis of dynamic alignment of field lines by diffusive mechanisms, which predicts just such an effect.

In analyzing the tube curvature we see that two dominant processes are the straightening of tubes by the stretching strain creating them, and convection by strong vortex tubes. The numerics show that both are important. Since the first is particularly strong for long, coherent stretching strains that also create strong tubes, we expect that strong tubes will be straighter.

ACKNOWLEDGMENTS

We thank Steve Arendt, Bob Kerr, Reuven Zeitak, and Ellen Zweibel for stimulating discussions and especially Barak Galanti, with whom we developed the routines for calculating the geometric quantities. A.B. thanks The Weizmann Institute for Science, where part of this work was carried out, for its hospitality.

This research has been supported in part by the U.S.–Israel Binational Science Foundation and the Israel Academy of Sciences and Humanities. Most of the computations have been performed on the Cray-3 at the National Center for Atmospheric Research. The National Center for Atmospheric Research is sponsored by the National Science Foundation.

[1] S. Kida, S. Yanase, and J. Mizushima, Phys. Fluids A **3**, 457 (1991).
[2] Å. Nordlund, A. Brandenburg, R. L. Jennings, M. Rieutord, J. Ruokolainen, R. F. Stein, and I. Tuominen, Astrophys. J. **392**, 647 (1992).
[3] D. Galloway and U. Frisch, Geophys. Astrophys. Fluid Dyn. **36**, 53 (1986).
[4] E. D. Siggia, J. Fluid Mech. **107**, 375 (1981).
[5] R. M. Kerr, J. Fluid Mech. **153**, 31 (1985).
[6] A. Vincent and M. Meneguzzi, J. Fluid Mech. **225**, 1 (1991).
[7] H. Tennekes, Phys. Fluids **11**, 669 (1968).
[8] See, e.g., A. Pouquet and G. S. Patterson, J. Fluid Mech. **85**, 305 (1978).
[9] J. Jiménez, A. A. Wray, P. G. Saffman, and R. S. Rogallo, J. Fluid Mech. **255**, 65 (1993).
[10] N. O. Weiss, Proc. R. Soc. London Ser. A **293**, 310 (1966).
[11] D. J. Galloway, M. R. E. Proctor, and N. O. Weiss, Nature **266**, 686 (1977).
[12] G. S. Golitsyn, Sov. Phys. Dokl. **5**, 536 (1960).
[13] R. H. Kraichnan and S. Nagarajan, Phys. Fluids **10**, 859 (1967).
[14] P. Constantin, I. Procaccia, and D. Segel, "Creation and dynamics of vortex tubes in three-dimensional turbulence," Phys. Rev. E (in press).
[15] I. T. Drummond and W. Münch, J. Fluid Mech. **225**, 529 (1991).
[16] The routines for calculating the local geometric quantities have been compared for periodic ABC and Taylor–Green flows with spectral routines; the agreement is excellent.
[17] For reasons of numerical accuracy we express the torsion in terms of **B** using $T=(\mathbf{f}\cdot\mathbf{g})\mathbf{B}^2/(\mathbf{f}\times\mathbf{B})^2$, where $\mathbf{f}\equiv\mathbf{B}\times\mathbf{h}$, $\mathbf{g}\equiv(\mathbf{h}\cdot\nabla)\mathbf{B}+B_jB_k\partial_j\partial_k\mathbf{B}$, and $\mathbf{h}\equiv(\mathbf{B}\cdot\nabla)\mathbf{B}$.